Acta Cryst E CRYSTALLOGRAPHIC COMMUNICATIONS

ISSN 2056-9890

Synthesis, crystal structure and Hirshfeld analysis of *trans*-bis{(2*E*)-*N*-phenyl-2-[(2*E*)-3-phenyl-2-propen-1-ylidene]hydrazinecarbothioamidato-κ^2N^1,S}-palladium(II)

Ana Paula Lopes de Melo,[a] Bianca Barreto Martins,[a] Leandro Bresolin,[a]* Bárbara Tirloni[b] and Adriano Bof de Oliveira[c]

[a]Escola de Química e Alimentos, Universidade Federal do Rio Grande, Av. Itália km 08, Campus Carreiros, 96203-900 Rio Grande-RS, Brazil, [b]Departamento de Química, Universidade Federal de Santa Maria, Av. Roraima s/n, Campus Universitário, 97105-900 Santa Maria-RS, Brazil, and [c]Departamento de Química, Universidade Federal de Sergipe, Av. Marcelo Deda Chagas s/n, Campus Universitário, 49107-230 São Cristóvão-SE, Brazil. *Correspondence e-mail: leandro_bresolin@yahoo.com.br

Received 4 September 2023
Accepted 2 October 2023

Edited by A. Briceno, Venezuelan Institute of Scientific Research, Venezuela

Keywords: palladium(II) thiosemicarbazone complex; cinnamaldehyde 4-phenylthiosemicarbazone; Hirshfeld surface analysis; crystal structure.

CCDC reference: 2163054

Supporting information: this article has supporting information at journals.iucr.org/e

The reaction of (2*E*)-*N*-phenyl-2-[(2*E*)-3-phenyl-2-propen-1-ylidene]hydrazinecarbothioamide (common name: cinnamaldehyde-4-phenylthiosemicarbazone) deprotonated with NaOH in ethanol with an ethanolic suspension of Pd^{II} chloride in a 2:1 molar ratio yielded the title compound, $[Pd(C_{16}H_{14}N_3S)_2]$. The anionic ligands act as metal chelators, κ^2N^1S-donors, forming five-membered rings with a *trans*-configuration. The Pd^{II} ion is fourfold coordinated in a slightly distorted square-planar geometry. For each ligand, one H···S and one H···N intramolecular interactions are observed, with *S*(5) and *S*(6) graph-set motifs. Concerning the H···S interactions, the coordination sphere resembles a hydrogen-bonded macrocyclic environment-type. In the crystal, the complexes are linked *via* pairs of H···S interactions, with graph-set motif $R_2^2(8)$, and building a mono-periodic hydrogen-bonded ribbon along [001]. The Hirshfeld surface analysis indicates that the major contributions for the crystal cohesion are: H···H (45.3%), H···C/C···H (28.0%), H···S/S···H (8.0%) and H···N/N···H (7.4%).

1. Chemical context

As far as we know, the thiosemicarbazone chemistry can be traced back to the beginning of the 1900s, when a thiosemicarbazide derivative, $H_2N-N(H)C(=S)NR_1R_2$, was used as chemical reagent for the characterization of aldehydes and ketones, $R_3R_4C=O$. It was pointed out that the main product of the characterization reaction was a thiosemicarbazone derivative, $R_3R_4C=N-N(H)C(=S)NR_1R_2$ (Freund & Schander, 1902). In the second half of the 1950s, the use of 4-phenylthiosemicarbazide as reagent for the characterization of cinnamaldehyde was reported and the cinnamaldehyde 4-phenylthiosemicarbazone molecule, the ligand of the title compound, was the major product of the reaction (Tišler, 1956).

From early times, as a product of qualitative analysis reactions in the organic chemistry, thiosemicarbazone chemistry emerged as a large class of compounds present in a wide range of scientific disciplines. For example, the cinnamaldehyde 4-phenylthiosemicarbazone derivative shows anti-corrosion activity for copper in nitric acid media (Mostafa, 2000).

One of the most important applications of thiosemicarbazone derivatives is in coordination chemistry. The N—N(H)—C(=S) fragment can be easily deprotonated and

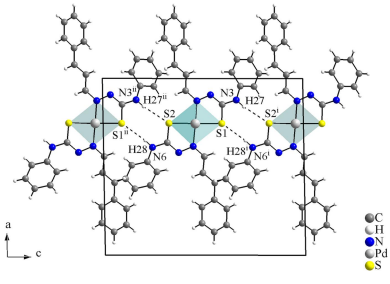

the negative charge is then delocalized over the N—N—C—S entity, which enables chemical bonding with many different metal centers, with different Lewis acidity, and a diversity of coordination modes, *e.g.*, chelating and bridging. Complexes with anionic thiosemicarbazone derivatives are more common as a result of the charge density and the geometry adopted by the ligands (Lobana *et al.*, 2009).

Many complexes with thiosemicarbazone ligands show relevant biological activity. For example, Pd^{II} heteroleptic complexes with a cinnamaldehyde-thiosemicarbazone derivative turned out to be very active on *in vitro* Human Topoisomerase IIα inhibition, a biological target of prime importance for cancer research (Rocha *et al.*, 2019). Other Pd^{II} homoleptic and heteroleptic complexes with cinnamaldehyde-thiosemicarbazone as ligands were reported to be active against five human cancer cell lines *in vitro*: colon (Caco-2), cervix (HeLa), hepatocellular (HepG2), breast (MCF-7) and prostate (PC-3) (Nyawadea *et al.*, 2021). Finally, Ni^{II} homoleptic cinnamaldehyde-4-ethylthiosemicarbazone and cinnamaldehyde-4-methylthiosemicarbazone derivative complexes showed, also in *in vitro* assays, inhibition of cell growth for two selected human tumour cell lines: breast (MCF-7) and lung (A549) (Farias *et al.*, 2021).

Another interesting approach for cinnamaldehyde-thiosemicarbazone chemistry is the synthesis of nanostructured materials through thermal and solvothermal decomposition techniques, where thiosemicarbazone complexes are employed as single-molecule precursors. It was reported that the thermal and solvothermal decomposition of ZnL_2 and $ZnCl_2(LH)_2$ homo- and heteroleptic complexes results in the formation of ZnS nanocrystallites (for this section only, L = the anionic form of cinnamaldehyde-thiosemicarbazone and LH = the neutral form of it) (Palve & Garje, 2011). Similarly, Cd^{II} heteroleptic complexes $CdCl_2(LH)_2$ and $CdI_2(LH)_2$ were used as starting materials to obtain CdS nanoparticles (Pawar *et al.*, 2016) and CoS or Co_9S_8 nanocrystallites were synthesized from CoL_2 and $CoCl_2(LH)_2$ homo- and heteroleptic complexes (Pawar & Garje, 2015).

Motivated by the bioinorganic chemistry and materials science of the cinnamaldehyde-thiosemicarbazone complexes, we report herein the synthesis, crystal structure and Hirshfeld analysis of a new Pd^{II} homoleptic complex where the cinnamaldehyde-4-phenylthiosemicarbazone molecules act as anionic ligands.

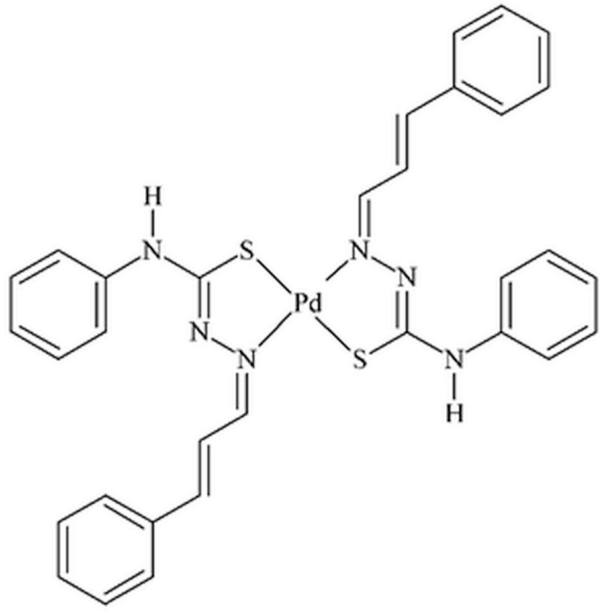

2. Structural commentary

The asymmetric unit comprises one molecule of the title compound, with all atoms being located in general positions (Fig. 1). The complex consists of one Pd^{II} metal center and two deprotonated cinnamaldehyde-4-phenylthiosemicarbazone ligands, which act as metal chelators, forming five-membered metallarings. The ligands are coordinated through N and S atoms in a *trans*-configuration, κ^2N^1S-donors, and the N1—Pd1—N4 and the S1—Pd1—S2 angles are 178.31 (6) and 177.57 (2)°, respectively. The metal ion is fourfold coordinated in a slightly distorted square-planar geometry. The maximum deviation from the mean plane through the Pd1/N1/N4/S1/S2 fragment is 0.0227 (5) Å for Pd1 and the r.m.s. for the selected atoms is 0.0151 Å. Concerning the geometry of the N—N—C—S entities, the N1—N2—C10—S1 torsion angle is

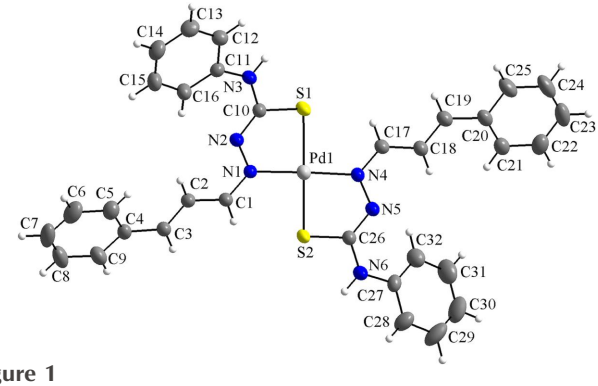

Figure 1
The molecular structure of the title compound, showing the atom labeling and displacement ellipsoids drawn at the 40% probability level.

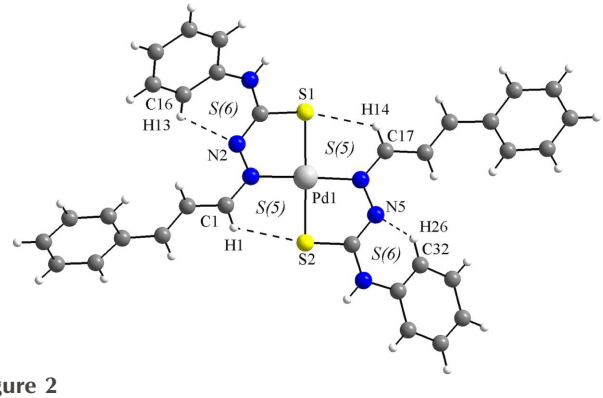

Figure 2
C—H···S and C—H···N hydrogen intramolecular interactions of the title compound (dashed lines), forming rings of $S(5)$ and $S(6)$ graph-set motifs. A hydrogen-bonded macrocyclic coordination environment-type can be suggested for the Pd^{II} metal center.

Table 1
Hydrogen-bond geometry (Å, °).

D—H···A	D—H	H···A	D···A	D—H···A
C1—H1···S2	0.93	2.60	3.230 (2)	126
C16—H13···N2	0.93	2.32	2.887 (3)	119
C17—H14···S1	0.93	2.72	3.355 (2)	126
C32—H26···N5	0.93	2.39	2.911 (3)	115
N3—H27···S2^{i}	0.86	2.63	3.4805 (18)	171
N6—H28···S1^{ii}	0.86	2.84	3.6554 (19)	159

Symmetry codes: (i) $x, -y+\frac{1}{2}, z+\frac{1}{2}$; (ii) $x, -y+\frac{1}{2}, z-\frac{1}{2}$.

0.6 (3)°, while N4—N5—C26—S2 is −0.4 (3)°. Both of the ligands are non-planar, with the angle between the mean planes through the C4–C9 and the C11–C16 aromatic rings being 15.7 (1)°, while that between the C20–C25 and the C27–C32 rings is 45.5 (8)°.

Four intramolecular hydrogen-bonding interactions are observed (Fig. 2, Table 1): C1—H1···S2 and C17—H14···S1, with graph-set motif $S(5)$, and C16—H13···N2 and C32—H26···N5, with graph-set motif $S(6)$. Considering the $S(5)$ rings, a hydrogen-bonded macrocyclic coordination environment-type can be suggested for the Pd^{II} metal center, while the $S(6)$ rings contribute to the stabilization of the molecular structure.

Finally, the anionic form of the ligands was assigned because of the absence of hydrazinic H atoms and the change in the bond lengths of the N—N—C—S entities. For the neutral or free, *i.e.*, non-coordinating thiosemicarbazones, the N—N and C—S bonds have lengths of double-bond character, while the N—C bond shows lengths of single-bond type, which can be written as a N═N(H)—C═S fragment. When the acidic H atom of the hydrazinic fragment is removed, the negative charge is delocalized over the N—N—C—S chain and the bond lengths change to intermediate values. Thus, the N—N and the C—S bond lengths assume single-bond character, being longer, and the N—C bond lengths assume double-bond character, being shorter. Information about the bond lengths

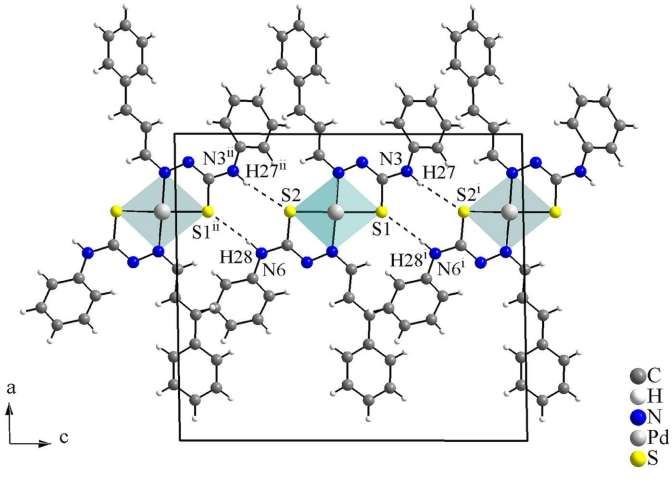

Figure 3
Crystal structure section of the title compound viewed along the *b*-axis. The N—H···S interactions are drawn as dashed lines, forming rings of $R_2^2(8)$ graph-set motif and linking the molecules along the *c*-axis. [Symmetry codes: (i) $x, -y+\frac{1}{2}, z+\frac{1}{2}$; (ii) $x, -y+\frac{1}{2}, z-\frac{1}{2}$.]

Table 2
Bond lengths (Å) for the N—N—C—S entities in cinnamaldehyde-4-phenylthiosemicarbazone structures: as a neutral molecule and as an anionic ligand.

	N—N	N—C	C—S
$C_{16}H_{15}N_3S$[a,c]	1.369 (2)	1.354 (2)	1.6704 (19)
$Ni(C_{16}H_{14}N_3S)_2$[b,c]	1.405 (5)	1.301 (6)	1.730 (5)
$Pd(C_{16}H_{14}N_3S)_2$[b,d]	1.390 (2)	1.293 (2)	1.7520 (19)
	1.393 (2)	1.291 (2)	1.7328 (19)

Notes: (*a*) Neutral, non-coordinated form of the cinnamaldehyde 4-phenylthiosemicarbazone; (*b*) anionic, coordinated form of the cinnamaldehyde 4-phenylthiosemicarbazone; (*c*) Song *et al.* (2014); (*d*) this work.

of the N—N—C—S entities for the cinnamaldehyde-4-phenylthiosemicarbazone molecule, $C_{16}H_{15}N_3S$, and the $Ni(C_{16}H_{14}N_3S)_2$ (Song *et al.*, 2014) and $Pd(C_{16}H_{14}N_3S)_2$ complexes, this work, are summarized in Table 2. These data are in agreement with reported bond lengths values for thiosemicarbazone derivatives (Oliveira *et al.*, 2014).

3. Supramolecular features

In the crystal, the molecules are connected *via* pairs of N—H···S interactions with graph-set motif $R_2^2(8)$, forming a mono-periodic hydrogen-bonded ribbon along [001] (Fig. 3, Table 1).

The Hirshfeld surface analysis (Hirshfeld, 1977) of the crystal structure was performed with *Crystal Explorer* (Wolff *et al.*, 2012). The graphical representations of the Hirshfeld surface for the title compound are represented using a ball-and-stick model with transparency, in two side-views and

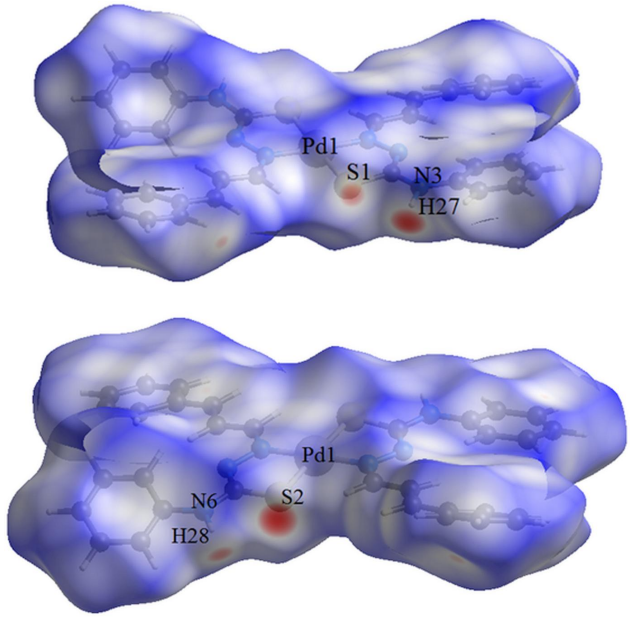

Figure 4
Two side-views in separate figures of the Hirshfeld surface graphical representation (d_{norm}) for the title compound. The surface is drawn with transparency and simplified for clarity and the regions with strongest intermolecular interactions are shown in magenta. [d_{norm} range: −0.289 to 1.415]

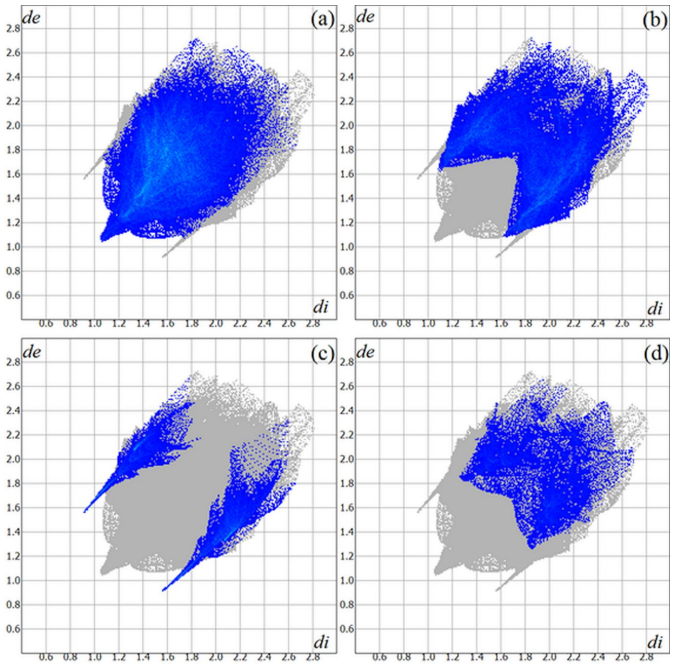

Figure 5
The Hirshfeld surface two-dimensional fingerprint plot for the title compound showing the (*a*) H···H, (*b*) H···C/C···H, (*c*) H···S/S···H and (*d*) H···N/N···H contacts in detail (cyan dots). The contributions of the interactions to the crystal cohesion amount to 45.3, 28.0, 8.0 and 7.4%, respectively. The d_i (*x*-axis) and the d_e (*y*-axis) values are the closest internal and external distances from given points on the Hirshfeld surface (in Å).

separate figures for clarity (Fig. 4). The locations of the strongest intermolecular contacts, *i.e*, the regions around the S1, H27, S2 and H28 atoms, are indicated in magenta. These atoms are those involved in the N—H···S intermolecular interactions represented in the previous figure (Fig. 3): N3—H27···S2^{i} and N6—H28···S1^{ii} [symmetry codes: (i) x, $-y+\frac{1}{2}$, $z+\frac{1}{2}$; (ii) x, $-y+\frac{1}{2}$, $z-\frac{1}{2}$]. The Hirshfeld surface analysis of the crystal structure also indicates that the most relevant intermolecular interactions for crystal packing are the following: (*a*) H···H (45.3%), (*b*) H···C/C···H (28.0%), (*c*) H···S/S···H (8.0%) and (*d*) H···N/N···H (7.4%). The contributions to the crystal packing are shown as two-dimensional Hirshfeld surface fingerprint plots with cyan dots (Fig. 5). The d_i (*x*-axis) and the d_e (*y*-axis) values are the closest internal and external distances from given points on the Hirshfeld surface (in Å).

4. Database survey

To the best of our knowledge and using database tools such as *SciFinder*^{TM} (Chemical Abstracts Service, 2023), there is only one report of the crystal structure of a compound bearing cinnamaldehyde-4-phenylthiosemicarbazone as non-coordinated molecule ($C_{16}H_{15}N_3S$) and as a ligand, *viz*. in the homoleptic [Ni($C_{16}H_{14}N_3S$)$_2$] complex (Song *et al.*, 2014). The asymmetric unit of the reference coordination compound consists of one Ni^{II} ion, which lies on an inversion center, and two deprotonated cinnamaldehyde-4-phenylthiosemicarba-

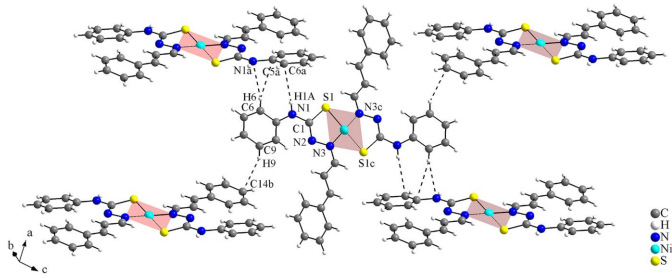

Figure 6
Part of the crystal structure of the reference compound, the centrosymmetric [Ni($C_{16}H_{14}N_3S$)$_2$] complex (Song *et al.*, 2014). The H···C and H···N intermolecular contacts are drawn as dashed lines and the figure is simplified for clarity. [Symmetry codes: (*a*) $-x+1$, $y+\frac{1}{2}$, $-z+\frac{1}{2}$; (*b*) $-x$, $y+\frac{1}{2}$, $-z+\frac{1}{2}$; (*c*) $-x+1$, $-y+2$, $-z+1$.]

zone ligands, in one of which the atoms are general positions while the second is generated by symmetry (Fig. 6) [symmetry code: (*c*) $-x+1$, $-y+2$, $-z+1$]. The negative charge of the ligand was assigned by the absence of a hydrazinic H atom and the bond distances in the N—N—C—S chain (please see the remarks in the *Structural commentary* section of this work and also Table 2). The coordination environment of the Ni^{II} complex is quite similar to that for the Pd^{II} metal center of the title compound: the anionic ligands act as metal chelators, κ^2N^1S-donors, with N and S atoms in *trans*-positions (180°), the metal center is fourfold coordinated in a square-planar geometry and the N—N—C—S entity torsion angle is 1.5 (6)°.

Although the coordination sphere of the Pd^{II} title compound and the Ni^{II} analogue compound are similar, the supramolecular arrangement of the complexes is totally different. In the crystal, the molecules of the centrosymmetric Ni^{II} coordination compound are linked into a three-dimensional hydrogen-bonded network. The H···S intermolecular interactions, like those observed in the Pd^{II} complex (Fig. 3), are not present in this case and only very weak H···C and H···N intermolecular contacts are noted. The values for the hydrogen-bonding of the asymmetric part of the complex amount to: C6—H6···C5^{a} = 2.90 (5) Å, C6—H6···N1^{a} = 2.73 (5) Å, C9—H9···C14^{b} = 2.86 (6) Å and N1—H1*A*···C6^{a} = 2.90 (7) Å [symmetry codes: (*a*) $-x+1$, $y+\frac{1}{2}$, $-z+\frac{1}{2}$; (*b*) $-x$, $y+\frac{1}{2}$, $-z+\frac{1}{2}$] (Fig. 6). The H···C and H···N distances are slightly above the sum of the van der Waals radii for the respective atoms (Bondi, 1964; Rowland & Taylor, 1996) and they are the only intermolecular contacts observed for the supramolecular structure of the Ni^{II} complex.

The Hirshfeld surface analysis (Hirshfeld, 1977) of the crystal structure of the Ni^{II} coordination compound was also performed with *CrystalExplorer* (Wolff *et al.*, 2012). The graphical representation of the Hirshfeld surface is represented using a ball-and-stick model with transparency and the locations of the strongest intermolecular contacts are draw in magenta, *i.e.*, the regions around the C6, H6, N1, H1*A*, H9$^{\#}$ and C14$^{\#}$ atoms (Fig. 7) [symmetry code: (#) $-x+1$, $-y+2$, $-z+1$]. These data are in agreement with the weak H···C and H···N intermolecular contacts observed in the previous figure (Fig. 6). The contributions to the crystal packing are shown as

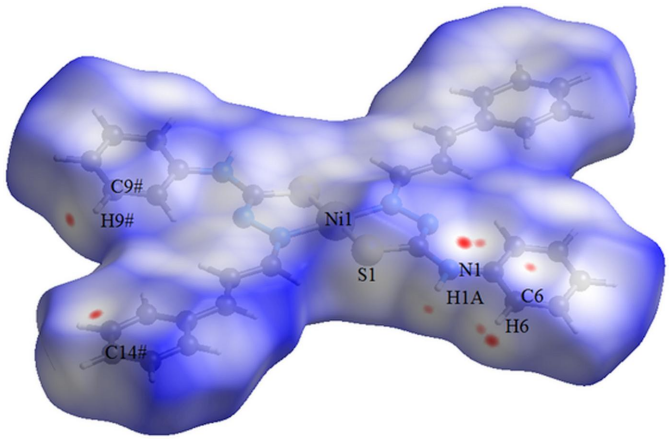

Figure 7
The Hirshfeld surface graphical representation [d_{norm} range: −0.045 to 1.492] for the centrosymmetric Ni^{II} complex (Song *et al.*, 2014). The surface is drawn with transparency and simplified for clarity. The surface regions with strongest intermolecular contacts are shown in magenta. [Symmetry code: (#) $-x+1, -y+2, -z+1$.]

two-dimensional Hirshfeld surface fingerprint plots with cyan dots (Fig. 8). The Hirshfeld surface analysis of the crystal structure also suggests that the most important intermolecular interactions for crystal packing are the following: (*a*) H···H (47.4%), (*b*) H···C/C···H (27.6%), (*c*) H···N/N···H (7.0%) and (*d*) H···S/S···H (6.5%). The d_i (*x*-axis) and the d_e (*y*-axis) values are the closest internal and external distances from given points on the Hirshfeld surface contacts (in Å). While for the Pd^{II} title compound and the Ni^{II} reference compound the most important intermolecular contacts are H···H and the H···C/C···H, the order of importance changes for the H···S/S···H and H···N/N···H contacts. For the crystal packing of the Pd^{II} complex, the H···S/S···H contacts are more important then H···N/N···H contacts, while for the Ni^{II} complex this order is the opposite.

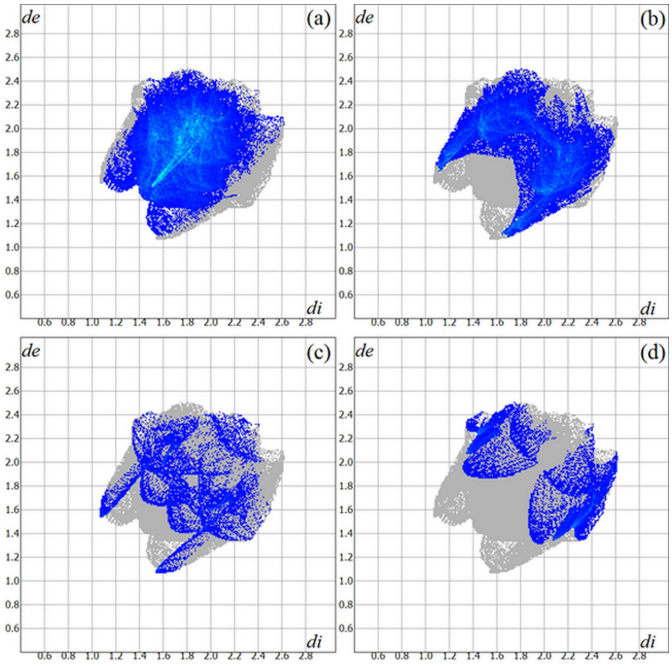

Figure 8
The Hirshfeld surface two-dimensional fingerprint plot for the Ni^{II} coordination compound (Song *et al.*, 2014) showing the (*a*) H···H, (*b*) H···C/C···H, (*c*) H···N/N···H and (*d*) H···S/S···H contacts in detail (cyan dots). The contributions of the interactions to the crystal cohesion amount to 47.4, 27.6, 7.0 and 6.5%, respectively. The d_i (*x*-axis) and the d_e (*y*-axis) values are the closest internal and external distances from given points on the Hirshfeld surface (in Å).

Table 3
Experimental details.

Crystal data	
Chemical formula	$[Pd(C_{16}H_{14}N_3S)_2]$
M_r	667.12
Crystal system, space group	Monoclinic, $P2_1/c$
Temperature (K)	299
a, *b*, *c* (Å)	15.084 (5), 11.418 (4), 17.097 (6)
β (°)	91.097 (9)
V (Å^3)	2944.0 (16)
Z	4
Radiation type	Mo $K\alpha$
μ (mm^{-1})	0.81
Crystal size (mm)	0.25 × 0.18 × 0.11
Data collection	
Diffractometer	Bruker D8 Venture Photon 100 area detector diffractometer
Absorption correction	Multi-scan (*SADABS*; Krause *et al.*, 2015)
T_{min}, T_{max}	0.699, 0.746
No. of measured, independent and observed [$I > 2\sigma(I)$] reflections	87933, 7344, 6204
R_{int}	0.042
(sin $\theta/\lambda)_{max}$ (Å^{-1})	0.668
Refinement	
$R[F^2 > 2\sigma(F^2)]$, $wR(F^2)$, S	0.026, 0.063, 1.05
No. of reflections	7344
No. of parameters	370
H-atom treatment	H-atom parameters constrained
$\Delta\rho_{max}$, $\Delta\rho_{min}$ (e Å^{-3})	0.34, −0.50

Computer programs: *APEX3* and *SAINT* (Bruker, 2015), *SHELXT2014/5* (Sheldrick, 2015*a*), *SHELXL2018/3* (Sheldrick, 2015*b*), *DIAMOND* (Brandenburg, 2006), *CrystalExplorer* (Wolff *et al.*, 2012), *WinGX* (Farrugia, 2012), *publCIF* (Westrip, 2010) and *enCIFer* (Allen *et al.*, 2004).

5. Synthesis and crystallization

The starting materials are commercially available and were used without further purification. The synthesis of the ligand was adapted from a previously reported procedure (Freund & Schander, 1902; Tišler, 1956). Cinnamaldehyde-4-phenylthiosemicarbazone was dissolved in ethanol (4 mmol, 50 mL) and deprotonated with one pellet of NaOH with stirring maintained for 2 h until the solution turned yellow. Simultaneously, an ethanolic suspension of palladium(II) chloride (2 mmol, 50 mL) was prepared under continuous stirring. A yellow-colored mixture of the ethanolic solution and the ethanolic suspension was maintained with stirring at room temperature for 8 h, until the $PdCl_2$ was consumed. Orange single crystals suitable for X-ray diffraction were obtained by the slow evaporation of the solvent.

6. Refinement

Crystal data, data collection and structure refinement details are summarized in Table 3. Hydrogen atoms were located in a difference-Fourier map, but were positioned with idealized geometry and refined isotropically using a riding model (HFIX command), with U_{iso}(H) = 1.2 U_{eq}(C, N), and with C—H = 0.93 Å and N—H = 0.86 Å.

Acknowledgements

APLM thanks CAPES for the award of a PhD scholarship. The authors thank the Department of Chemistry of the Federal University of Santa Maria/Brazil for the access to the X-ray diffraction facility.

Funding information

Funding for this research was provided by: Coordenação de Aperfeiçoamento de Pessoal de Nível Superior – Brazil (CAPES), Finance code 001.

References

Allen, F. H., Johnson, O., Shields, G. P., Smith, B. R. & Towler, M. (2004). *J. Appl. Cryst.* **37**, 335–338.

Bondi, A. (1964). *J. Phys. Chem.* **68**, 441–451.

Brandenburg, K. (2006). *DIAMOND*. Crystal Impact GbR, Bonn, Germany.

Bruker (2015). *APEX3* and *SAINT*. Bruker AXS Inc., Madison, Wisconsin, USA.

Chemical Abstracts Service (2023). Columbus, Ohio, USA (accessed *via* SciFinder on September 1, 2023).

Farias, R. L., Polez, A. M. R., Silva, A. D. E. S., Zanetti, R. D., Moreira, M. B., Batista, V. S., Reis, B. L., Nascimento-Júnior, N. M., Rocha, F. V., Lima, M. A., Oliveira, A. B., Ellena, J., Scarim, C. B., Zambom, C. R., Brito, L. D., Garrido, S. S., Melo, A. P. L., Bresolin, L., Tirloni, B., Pereira, J. C. M. & Netto, A. V. G. (2021). *Mater. Sci. Eng. C*, **121**, 111815, 1–12.

Farrugia, L. J. (2012). *J. Appl. Cryst.* **45**, 849–854.

Freund, M. & Schander, A. (1902). *Ber. Dtsch. Chem. Ges.* **35**, 2602–2606.

Hirshfeld, H. L. (1977). *Theor. Chim. Acta*, **44**, 129–138.

Krause, L., Herbst-Irmer, R., Sheldrick, G. M. & Stalke, D. (2015). *J. Appl. Cryst.* **48**, 3–10.

Lobana, T. S., Sharma, R., Bawa, G. & Khanna, S. (2009). *Coord. Chem. Rev.* **253**, 977–1055.

Mostafa, H. A. (2000). *Electrochim. Acta*, **18**, 45–53.

Nyawadea, E. A., Sibuyi, N. R. S., Meyer, M., Lalancette, R. & Onani, M. O. (2021). *Inorg. Chim. Acta*, **515**, 120036, 1–10.

Oliveira, A. B. de, Feitosa, B. R. S., Näther, C. & Jess, I. (2014). *Acta Cryst.* E**70**, 101–103.

Palve, A. M. & Garje, S. S. (2011). *J. Cryst. Growth*, **326**, 157–162.

Pawar, A. S. & Garje, S. S. (2015). *Bull. Mater. Sci.* **38**, 1843–1850.

Pawar, A. S., Masikane, S. C., Mlowe, S., Garje, S. S. & Revaprasadu, N. (2016). *Eur. J. Inorg. Chem.* pp. 366–372.

Rocha, F. V., Farias, R. L., Lima, M. A., Batista, V. S., Nascimento-Júnior, N. M., Garrido, S. S., Leopoldino, A. M., Goto, R. N., Oliveira, A. B., Beck, J., Landvogt, C., Mauro, A. E. & Netto, A. V. G. (2019). *J. Inorg. Biochem.* **199**, 110725, 1–9.

Rowland, R. S. & Taylor, R. (1996). *J. Phys. Chem.* **100**, 7384–7391.

Sheldrick, G. M. (2015*a*). *Acta Cryst.* A**71**, 3–8.

Sheldrick, G. M. (2015*b*). *Acta Cryst.* C**71**, 3–8.

Song, J., Zhu, F., Wang, H. & Zhao, P. (2014). *Spectrochim. Acta A Mol. Biomol. Spectrosc.* **129**, 227–234.

Tišler, M. (1956). *Z. Anal. Chem.* **149**, 164–172.

Westrip, S. P. (2010). *J. Appl. Cryst.* **43**, 920–925.

Wolff, S. K., Grimwood, D. J., McKinnon, J. J., Turner, M. J., Jayatilaka, D. & Spackman, M. A. (2012). *Crystal Explorer 3.1*. University of Western Australia, Australia.

supporting information

Acta Cryst. (2023). E**79**, 993-998 [https://doi.org/10.1107/S2056989023008654]

Synthesis, crystal structure and Hirshfeld analysis of *trans*-bis{(2*E*)-*N*-phenyl-2-[(2*E*)-3-phenyl-2-propen-1-ylidene]hydrazinecarbothioamidato-κ^2N^1,S}palladium(II)

Ana Paula Lopes de Melo, Bianca Barreto Martins, Leandro Bresolin, Bárbara Tirloni and Adriano Bof de Oliveira

Computing details

Data collection: *APEX3* (Bruker, 2015); cell refinement: *SAINT* (Bruker, 2015); data reduction: *SAINT* (Bruker, 2015); program(s) used to solve structure: *SHELXT2014/5* (Sheldrick, 2015*a*); program(s) used to refine structure: *SHELXL2018/3* (Sheldrick, 2015*b*); molecular graphics: *DIAMOND* (Brandenburg, 2006), *CrystalExplorer* (Wolff *et al.*, 2012); software used to prepare material for publication: *WinGX* (Farrugia, 2012), *publCIF* (Westrip, 2010) and *enCIFer* (Allen *et al.*, 2004).

***trans*-Bis{(2*E*)-*N*-phenyl-2-[(2*E*)-3-phenyl-2-propen-1-ylidene]hydrazinecarbothioamidato-κ^2N^1,S}palladium(II)**

Crystal data

$[Pd(C_{16}H_{14}N_3S)_2]$
M_r = 667.12
Monoclinic, $P2_1/c$
a = 15.084 (5) Å
b = 11.418 (4) Å
c = 17.097 (6) Å
β = 91.097 (9)°
V = 2944.0 (16) Å^3
Z = 4
$F(000)$ = 1360
D_x = 1.505 Mg m^{-3}
Mo $K\alpha$ radiation, λ = 0.71073 Å
Cell parameters from 9138 reflections
θ = 2.2–28.3°
μ = 0.81 mm^{-1}
T = 299 K
Block, orange
0.25 × 0.18 × 0.11 mm

Data collection

Bruker D8 Venture Photon 100 area detector diffractometer
Radiation source: microfocus X ray tube
φ and ω scans
Absorption correction: multi-scan (SADABS; Krause *et al.*, 2015)
T_{min} = 0.699, T_{max} = 0.746
87933 measured reflections
7344 independent reflections
6204 reflections with $I > 2\sigma(I)$
R_{int} = 0.042
θ_{max} = 28.4°, θ_{min} = 2.2°
h = −20→20
k = −15→15
l = −22→22

Refinement

Refinement on F^2
Least-squares matrix: full
$R[F^2 > 2\sigma(F^2)]$ = 0.026
$wR(F^2)$ = 0.063
S = 1.05
7344 reflections
370 parameters
0 restraints
Primary atom site location: structure-invariant direct methods

Hydrogen site location: inferred from neighbouring sites
H-atom parameters constrained

$w = 1/[\sigma^2(F_o^2) + (0.0241P)^2 + 1.5227P]$ where $P = (F_o^2 + 2F_c^2)/3$
$(\Delta/\sigma)_{max} = 0.003$
$\Delta\rho_{max} = 0.34$ e Å^{-3}
$\Delta\rho_{min} = -0.50$ e Å^{-3}

Special details

Geometry. All esds (except the esd in the dihedral angle between two l.s. planes) are estimated using the full covariance matrix. The cell esds are taken into account individually in the estimation of esds in distances, angles and torsion angles; correlations between esds in cell parameters are only used when they are defined by crystal symmetry. An approximate (isotropic) treatment of cell esds is used for estimating esds involving l.s. planes.

Fractional atomic coordinates and isotropic or equivalent isotropic displacement parameters (Å²)

	x	*y*	*z*	U_{iso}*/U_{eq}
C1	0.93114 (12)	0.25646 (18)	0.41478 (10)	0.0408 (4)
H1	0.911357	0.222755	0.368099	0.049*
C2	1.02188 (12)	0.29262 (18)	0.41878 (11)	0.0429 (4)
H2	1.042322	0.334403	0.462190	0.052*
C3	1.07777 (12)	0.26780 (19)	0.36174 (11)	0.0434 (4)
H3	1.054715	0.228656	0.318196	0.052*
C4	1.17186 (12)	0.29659 (18)	0.36156 (11)	0.0436 (4)
C5	1.20873 (15)	0.3801 (2)	0.41107 (14)	0.0566 (5)
H4	1.172634	0.422924	0.444057	0.068*
C6	1.29897 (17)	0.4000 (3)	0.41148 (17)	0.0738 (8)
H5	1.323135	0.457206	0.444183	0.089*
C7	1.35360 (16)	0.3362 (3)	0.36419 (19)	0.0765 (8)
H6	1.414532	0.348617	0.366163	0.092*
C8	1.31865 (17)	0.2555 (3)	0.31492 (18)	0.0745 (8)
H7	1.355493	0.212955	0.282440	0.089*
C9	1.22814 (15)	0.2358 (2)	0.31256 (14)	0.0613 (6)
H8	1.204591	0.181127	0.277638	0.074*
C10	0.85343 (12)	0.31504 (17)	0.59615 (10)	0.0377 (4)
C11	0.95766 (12)	0.42049 (17)	0.68829 (10)	0.0397 (4)
C12	0.95571 (14)	0.48633 (19)	0.75646 (11)	0.0466 (5)
H9	0.904012	0.489377	0.785175	0.056*
C13	1.02970 (15)	0.5473 (2)	0.78205 (13)	0.0559 (5)
H10	1.027308	0.591307	0.827731	0.067*
C14	1.10674 (15)	0.5437 (2)	0.74084 (14)	0.0584 (6)
H11	1.156512	0.585126	0.757969	0.070*
C15	1.10894 (14)	0.4777 (2)	0.67371 (14)	0.0597 (6)
H12	1.161063	0.474407	0.645610	0.072*
C16	1.03566 (13)	0.4160 (2)	0.64695 (12)	0.0516 (5)
H13	1.038671	0.371677	0.601430	0.062*
C17	0.55839 (12)	0.16720 (18)	0.50233 (11)	0.0416 (4)
H14	0.578917	0.185524	0.552491	0.050*
C18	0.46597 (12)	0.14045 (18)	0.49358 (11)	0.0429 (4)
H15	0.444566	0.115183	0.445071	0.052*
C19	0.40947 (13)	0.15030 (19)	0.55209 (12)	0.0472 (5)

H16	0.433316	0.172755	0.600361	0.057*
C20	0.31419 (13)	0.12958 (18)	0.54837 (12)	0.0454 (4)
C21	0.27211 (14)	0.0746 (2)	0.48604 (13)	0.0513 (5)
H17	0.305174	0.047797	0.444312	0.062*
C22	0.18134 (15)	0.0590 (2)	0.48519 (16)	0.0644 (6)
H18	0.153934	0.021536	0.442935	0.077*
C23	0.13142 (16)	0.0979 (3)	0.54540 (18)	0.0713 (8)
H19	0.070293	0.087173	0.544212	0.086*
C24	0.17159 (17)	0.1526 (3)	0.60741 (18)	0.0739 (8)
H20	0.137628	0.180199	0.648339	0.089*
C25	0.26240 (16)	0.1673 (2)	0.60978 (15)	0.0653 (6)
H21	0.289272	0.202928	0.653032	0.078*
C26	0.63696 (12)	0.14116 (18)	0.31857 (11)	0.0406 (4)
C27	0.52836 (12)	0.06730 (19)	0.21755 (12)	0.0456 (5)
C28	0.50883 (17)	0.0809 (2)	0.13948 (14)	0.0657 (7)
H22	0.547569	0.121832	0.107827	0.079*
C29	0.4319 (2)	0.0341 (3)	0.10764 (19)	0.0878 (10)
H23	0.418657	0.044846	0.054772	0.105*
C30	0.37560 (18)	−0.0272 (3)	0.1525 (2)	0.0837 (9)
H24	0.323855	−0.058496	0.130698	0.100*
C31	0.39511 (18)	−0.0431 (3)	0.23033 (19)	0.0803 (8)
H25	0.356585	−0.085945	0.261047	0.096*
C32	0.47140 (16)	0.0038 (2)	0.26388 (15)	0.0633 (6)
H26	0.484228	−0.007087	0.316803	0.076*
N1	0.87363 (10)	0.26614 (14)	0.47008 (8)	0.0375 (3)
N2	0.90767 (10)	0.31587 (16)	0.53850 (9)	0.0428 (4)
N3	0.87873 (10)	0.36111 (16)	0.66658 (9)	0.0442 (4)
H27	0.841082	0.352842	0.703313	0.053*
N4	0.61600 (10)	0.16837 (14)	0.44748 (9)	0.0383 (3)
N5	0.58090 (10)	0.13619 (16)	0.37463 (9)	0.0437 (4)
N6	0.61038 (11)	0.11296 (18)	0.24427 (9)	0.0521 (5)
H28	0.649000	0.124627	0.208750	0.063*
Pd1	0.74528 (2)	0.21629 (2)	0.46039 (2)	0.03379 (5)
S1	0.74605 (3)	0.25655 (5)	0.59231 (3)	0.04797 (12)
S2	0.74676 (3)	0.18416 (6)	0.32859 (3)	0.04861 (13)

Atomic displacement parameters (Å²)

	U^{11}	U^{22}	U^{33}	U^{12}	U^{13}	U^{23}
C1	0.0320 (9)	0.0589 (11)	0.0314 (9)	−0.0018 (8)	0.0020 (7)	−0.0014 (8)
C2	0.0327 (9)	0.0625 (12)	0.0337 (9)	−0.0045 (8)	−0.0002 (7)	0.0005 (8)
C3	0.0337 (9)	0.0606 (12)	0.0358 (9)	−0.0037 (9)	0.0015 (7)	0.0006 (9)
C4	0.0326 (9)	0.0575 (12)	0.0407 (10)	−0.0026 (8)	0.0018 (7)	0.0101 (9)
C5	0.0445 (12)	0.0656 (14)	0.0596 (13)	−0.0060 (10)	−0.0040 (10)	0.0032 (11)
C6	0.0551 (15)	0.0816 (18)	0.0838 (18)	−0.0223 (14)	−0.0209 (14)	0.0151 (15)
C7	0.0348 (12)	0.094 (2)	0.100 (2)	−0.0080 (13)	−0.0040 (13)	0.0419 (18)
C8	0.0416 (13)	0.097 (2)	0.0858 (19)	0.0078 (13)	0.0206 (13)	0.0207 (17)
C9	0.0445 (12)	0.0805 (17)	0.0594 (14)	−0.0030 (11)	0.0151 (10)	−0.0011 (12)

C10	0.0314 (9)	0.0475 (10)	0.0343 (9)	0.0002 (7)	0.0017 (7)	−0.0005 (7)
C11	0.0351 (9)	0.0486 (10)	0.0354 (9)	0.0000 (8)	−0.0029 (7)	0.0001 (8)
C12	0.0446 (11)	0.0557 (12)	0.0396 (10)	−0.0024 (9)	0.0016 (8)	−0.0032 (9)
C13	0.0578 (13)	0.0596 (13)	0.0499 (12)	−0.0054 (11)	−0.0067 (10)	−0.0103 (10)
C14	0.0443 (12)	0.0655 (14)	0.0650 (14)	−0.0103 (10)	−0.0128 (10)	−0.0005 (11)
C15	0.0341 (10)	0.0826 (17)	0.0624 (14)	−0.0034 (11)	0.0010 (10)	−0.0032 (12)
C16	0.0361 (10)	0.0735 (14)	0.0453 (11)	0.0009 (10)	0.0016 (8)	−0.0096 (10)
C17	0.0360 (9)	0.0542 (11)	0.0347 (9)	−0.0016 (8)	0.0036 (7)	−0.0037 (8)
C18	0.0356 (9)	0.0542 (11)	0.0392 (10)	−0.0007 (8)	0.0053 (8)	−0.0008 (8)
C19	0.0413 (10)	0.0586 (12)	0.0420 (10)	−0.0018 (9)	0.0078 (8)	−0.0009 (9)
C20	0.0390 (10)	0.0505 (11)	0.0471 (11)	0.0018 (8)	0.0116 (8)	0.0071 (9)
C21	0.0415 (11)	0.0609 (13)	0.0516 (12)	0.0024 (10)	0.0072 (9)	0.0081 (10)
C22	0.0468 (13)	0.0740 (16)	0.0722 (16)	−0.0050 (12)	−0.0071 (11)	0.0167 (13)
C23	0.0379 (12)	0.0804 (18)	0.096 (2)	0.0040 (12)	0.0149 (13)	0.0283 (16)
C24	0.0539 (14)	0.0804 (18)	0.089 (2)	0.0055 (13)	0.0362 (14)	0.0086 (16)
C25	0.0539 (14)	0.0782 (16)	0.0645 (15)	−0.0027 (12)	0.0246 (11)	−0.0050 (13)
C26	0.0315 (9)	0.0554 (11)	0.0351 (9)	−0.0013 (8)	0.0021 (7)	−0.0016 (8)
C27	0.0323 (9)	0.0553 (12)	0.0488 (11)	0.0009 (8)	−0.0040 (8)	−0.0101 (9)
C28	0.0631 (15)	0.0751 (16)	0.0582 (14)	−0.0127 (13)	−0.0205 (12)	0.0074 (12)
C29	0.084 (2)	0.095 (2)	0.083 (2)	−0.0132 (18)	−0.0477 (17)	0.0046 (17)
C30	0.0520 (15)	0.089 (2)	0.109 (2)	−0.0128 (14)	−0.0269 (16)	−0.0201 (18)
C31	0.0566 (15)	0.087 (2)	0.098 (2)	−0.0283 (14)	0.0074 (15)	−0.0243 (17)
C32	0.0520 (13)	0.0787 (16)	0.0592 (14)	−0.0154 (12)	0.0031 (11)	−0.0121 (12)
N1	0.0299 (7)	0.0523 (9)	0.0303 (7)	−0.0014 (6)	0.0009 (6)	−0.0023 (6)
N2	0.0324 (8)	0.0645 (10)	0.0316 (8)	−0.0058 (7)	0.0017 (6)	−0.0059 (7)
N3	0.0348 (8)	0.0659 (11)	0.0319 (8)	−0.0070 (8)	0.0045 (6)	−0.0067 (7)
N4	0.0304 (7)	0.0496 (9)	0.0349 (8)	−0.0023 (7)	0.0030 (6)	−0.0023 (7)
N5	0.0322 (8)	0.0646 (11)	0.0342 (8)	−0.0057 (7)	0.0027 (6)	−0.0055 (7)
N6	0.0341 (8)	0.0878 (14)	0.0346 (8)	−0.0110 (9)	0.0028 (7)	−0.0081 (8)
Pd1	0.02574 (7)	0.04563 (8)	0.03007 (7)	−0.00040 (5)	0.00212 (5)	−0.00124 (5)
S1	0.0344 (2)	0.0749 (3)	0.0349 (2)	−0.0119 (2)	0.00699 (18)	−0.0100 (2)
S2	0.0275 (2)	0.0866 (4)	0.0319 (2)	−0.0068 (2)	0.00370 (17)	−0.0071 (2)

Geometric parameters (Å, º)

C1—N1	1.300 (2)	C18—H15	0.9300
C1—C2	1.430 (3)	C19—C20	1.457 (3)
C1—H1	0.9300	C19—H16	0.9300
C2—C3	1.332 (3)	C20—C21	1.381 (3)
C2—H2	0.9300	C20—C25	1.389 (3)
C3—C4	1.457 (3)	C21—C22	1.380 (3)
C3—H3	0.9300	C21—H17	0.9300
C4—C5	1.385 (3)	C22—C23	1.361 (4)
C4—C9	1.389 (3)	C22—H18	0.9300
C5—C6	1.380 (3)	C23—C24	1.363 (4)
C5—H4	0.9300	C23—H19	0.9300
C6—C7	1.374 (4)	C24—C25	1.380 (3)
C6—H5	0.9300	C24—H20	0.9300

C7—C8	1.349 (4)	C25—H21	0.9300
C7—H6	0.9300	C26—N5	1.291 (2)
C8—C9	1.383 (3)	C26—N6	1.363 (2)
C8—H7	0.9300	C26—S2	1.7328 (19)
C9—H8	0.9300	C27—C28	1.370 (3)
C10—N2	1.293 (2)	C27—C32	1.384 (3)
C10—N3	1.362 (2)	C27—N6	1.410 (2)
C10—S1	1.7520 (19)	C28—C29	1.380 (3)
C11—C16	1.385 (3)	C28—H22	0.9300
C11—C12	1.388 (3)	C29—C30	1.351 (4)
C11—N3	1.413 (2)	C29—H23	0.9300
C12—C13	1.380 (3)	C30—C31	1.369 (4)
C12—H9	0.9300	C30—H24	0.9300
C13—C14	1.371 (3)	C31—C32	1.384 (3)
C13—H10	0.9300	C31—H25	0.9300
C14—C15	1.374 (3)	C32—H26	0.9300
C14—H11	0.9300	N1—N2	1.390 (2)
C15—C16	1.381 (3)	N1—Pd1	2.0217 (16)
C15—H12	0.9300	N3—H27	0.8600
C16—H13	0.9300	N4—N5	1.393 (2)
C17—N4	1.291 (2)	N4—Pd1	2.0333 (16)
C17—C18	1.432 (3)	N6—H28	0.8600
C17—H14	0.9300	Pd1—S2	2.2836 (9)
C18—C19	1.331 (3)	Pd1—S1	2.3016 (9)

N1—C1—C2	126.30 (17)	C25—C20—C19	119.0 (2)
N1—C1—H1	116.8	C22—C21—C20	120.5 (2)
C2—C1—H1	116.8	C22—C21—H17	119.7
C3—C2—C1	121.49 (18)	C20—C21—H17	119.7
C3—C2—H2	119.3	C23—C22—C21	120.9 (3)
C1—C2—H2	119.3	C23—C22—H18	119.6
C2—C3—C4	125.73 (19)	C21—C22—H18	119.6
C2—C3—H3	117.1	C22—C23—C24	119.6 (2)
C4—C3—H3	117.1	C22—C23—H19	120.2
C5—C4—C9	118.0 (2)	C24—C23—H19	120.2
C5—C4—C3	122.27 (19)	C23—C24—C25	120.3 (2)
C9—C4—C3	119.7 (2)	C23—C24—H20	119.8
C6—C5—C4	120.0 (2)	C25—C24—H20	119.8
C6—C5—H4	120.0	C24—C25—C20	120.8 (3)
C4—C5—H4	120.0	C24—C25—H21	119.6
C7—C6—C5	120.8 (3)	C20—C25—H21	119.6
C7—C6—H5	119.6	N5—C26—N6	119.74 (17)
C5—C6—H5	119.6	N5—C26—S2	125.25 (14)
C8—C7—C6	119.9 (2)	N6—C26—S2	115.00 (13)
C8—C7—H6	120.1	C28—C27—C32	119.5 (2)
C6—C7—H6	120.1	C28—C27—N6	116.4 (2)
C7—C8—C9	120.2 (3)	C32—C27—N6	123.9 (2)
C7—C8—H7	119.9	C27—C28—C29	120.3 (3)

C9—C8—H7	119.9	C27—C28—H22	119.9
C8—C9—C4	121.0 (3)	C29—C28—H22	119.9
C8—C9—H8	119.5	C30—C29—C28	120.6 (3)
C4—C9—H8	119.5	C30—C29—H23	119.7
N2—C10—N3	120.03 (17)	C28—C29—H23	119.7
N2—C10—S1	124.91 (14)	C29—C30—C31	119.7 (2)
N3—C10—S1	115.06 (13)	C29—C30—H24	120.2
C16—C11—C12	118.73 (18)	C31—C30—H24	120.2
C16—C11—N3	124.58 (18)	C30—C31—C32	120.9 (3)
C12—C11—N3	116.68 (17)	C30—C31—H25	119.6
C13—C12—C11	120.6 (2)	C32—C31—H25	119.6
C13—C12—H9	119.7	C31—C32—C27	119.0 (2)
C11—C12—H9	119.7	C31—C32—H26	120.5
C14—C13—C12	120.7 (2)	C27—C32—H26	120.5
C14—C13—H10	119.7	C1—N1—N2	113.95 (15)
C12—C13—H10	119.7	C1—N1—Pd1	124.60 (13)
C13—C14—C15	118.7 (2)	N2—N1—Pd1	121.45 (11)
C13—C14—H11	120.7	C10—N2—N1	114.18 (15)
C15—C14—H11	120.7	C10—N3—C11	129.63 (16)
C14—C15—C16	121.6 (2)	C10—N3—H27	115.2
C14—C15—H12	119.2	C11—N3—H27	115.2
C16—C15—H12	119.2	C17—N4—N5	113.40 (15)
C15—C16—C11	119.6 (2)	C17—N4—Pd1	125.56 (13)
C15—C16—H13	120.2	N5—N4—Pd1	121.01 (11)
C11—C16—H13	120.2	C26—N5—N4	114.13 (15)
N4—C17—C18	126.43 (17)	C26—N6—C27	129.03 (17)
N4—C17—H14	116.8	C26—N6—H28	115.5
C18—C17—H14	116.8	C27—N6—H28	115.5
C19—C18—C17	122.63 (19)	N1—Pd1—N4	178.31 (6)
C19—C18—H15	118.7	N1—Pd1—S2	95.66 (4)
C17—C18—H15	118.7	N4—Pd1—S2	82.94 (4)
C18—C19—C20	126.8 (2)	N1—Pd1—S1	82.92 (4)
C18—C19—H16	116.6	N4—Pd1—S1	98.45 (4)
C20—C19—H16	116.6	S2—Pd1—S1	177.57 (2)
C21—C20—C25	117.9 (2)	C10—S1—Pd1	95.74 (6)
C21—C20—C19	123.10 (18)	C26—S2—Pd1	96.65 (6)

N1—C1—C2—C3	172.9 (2)	C32—C27—C28—C29	1.5 (4)
C1—C2—C3—C4	−177.50 (19)	N6—C27—C28—C29	177.0 (3)
C2—C3—C4—C5	−17.8 (3)	C27—C28—C29—C30	−1.1 (5)
C2—C3—C4—C9	159.6 (2)	C28—C29—C30—C31	0.0 (5)
C9—C4—C5—C6	−0.8 (3)	C29—C30—C31—C32	0.6 (5)
C3—C4—C5—C6	176.7 (2)	C30—C31—C32—C27	−0.1 (4)
C4—C5—C6—C7	−1.2 (4)	C28—C27—C32—C31	−0.9 (4)
C5—C6—C7—C8	2.0 (4)	N6—C27—C32—C31	−176.0 (2)
C6—C7—C8—C9	−0.8 (4)	C2—C1—N1—N2	−0.7 (3)
C7—C8—C9—C4	−1.3 (4)	C2—C1—N1—Pd1	178.74 (16)
C5—C4—C9—C8	2.0 (4)	N3—C10—N2—N1	179.95 (17)

C3—C4—C9—C8	−175.5 (2)	S1—C10—N2—N1	0.6 (3)
C16—C11—C12—C13	0.8 (3)	C1—N1—N2—C10	−173.45 (18)
N3—C11—C12—C13	−179.92 (19)	Pd1—N1—N2—C10	7.1 (2)
C11—C12—C13—C14	−0.3 (3)	N2—C10—N3—C11	4.6 (3)
C12—C13—C14—C15	−0.3 (4)	S1—C10—N3—C11	−175.92 (16)
C13—C14—C15—C16	0.4 (4)	C16—C11—N3—C10	−18.5 (3)
C14—C15—C16—C11	0.2 (4)	C12—C11—N3—C10	162.2 (2)
C12—C11—C16—C15	−0.7 (3)	C18—C17—N4—N5	−2.1 (3)
N3—C11—C16—C15	−180.0 (2)	C18—C17—N4—Pd1	176.05 (16)
N4—C17—C18—C19	−174.5 (2)	N6—C26—N5—N4	−179.31 (18)
C17—C18—C19—C20	177.5 (2)	S2—C26—N5—N4	−0.4 (3)
C18—C19—C20—C21	13.0 (4)	C17—N4—N5—C26	177.55 (18)
C18—C19—C20—C25	−166.5 (2)	Pd1—N4—N5—C26	−0.7 (2)
C25—C20—C21—C22	0.5 (3)	N5—C26—N6—C27	−6.0 (4)
C19—C20—C21—C22	−178.9 (2)	S2—C26—N6—C27	175.02 (18)
C20—C21—C22—C23	0.3 (4)	C28—C27—N6—C26	160.2 (2)
C21—C22—C23—C24	−0.2 (4)	C32—C27—N6—C26	−24.6 (4)
C22—C23—C24—C25	−0.8 (4)	N2—C10—S1—Pd1	−6.03 (18)
C23—C24—C25—C20	1.7 (4)	N3—C10—S1—Pd1	174.54 (14)
C21—C20—C25—C24	−1.5 (4)	N5—C26—S2—Pd1	1.1 (2)
C19—C20—C25—C24	178.0 (2)	N6—C26—S2—Pd1	179.99 (15)

Hydrogen-bond geometry (Å, º)

D—H···*A*	*D*—H	H···*A*	*D*···*A*	*D*—H···*A*
C1—H1···S2	0.93	2.60	3.230 (2)	126
C16—H13···N2	0.93	2.32	2.887 (3)	119
C17—H14···S1	0.93	2.72	3.355 (2)	126
C32—H26···N5	0.93	2.39	2.911 (3)	115
N3—H27···S2^{i}	0.86	2.63	3.4805 (18)	171
N6—H28···S1^{ii}	0.86	2.84	3.6554 (19)	159

Symmetry codes: (i) *x*, −*y*+1/2, *z*+1/2; (ii) *x*, −*y*+1/2, *z*−1/2.